THE JOURNAL OF PHYSICAL CHEMISTRY C

Article

Enhancement of Photocatalytic Activity of Mesporous TiO Powders by Hydrothermal Surface Fluorination Treatment

Jiaguo Yu, Wenguang Wang, Bei Cheng, and Bao-Lian Su

J. Phys. Chem. C, **2009**, 113 (16), 6743-6750• Publication Date (Web): 31 March 2009

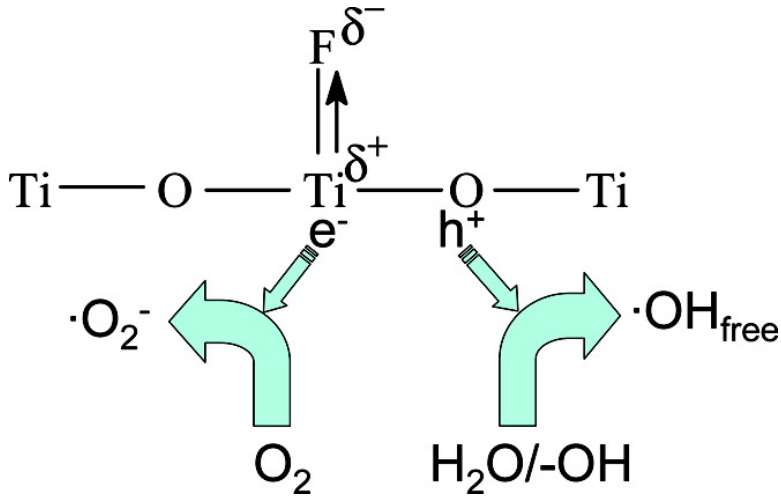

More About This Article

Additional resources and features associated with this article are available within the HTML version:

- Supporting Information
- Access to high resolution figures
- Links to articles and content related to this article
- Copyright permission to reproduce figures and/or text from this article

View the Full Text HTML

Enhancement of Photocatalytic Activity of Mesporous TiO_2 Powders by Hydrothermal Surface Fluorination Treatment

Jiaguo Yu,* Wenguang Wang, Bei Cheng, and Bao-Lian Su

State Key Laboratory of Advanced Technology for Material Synthesis and Processing, Wuhan University of Technology, Luoshi Road 122#, Wuhan 430070, People's Republic of China

Received: January 7, 2009

Mesporous surface-fluorinated TiO_2 ($F-TiO_2$) powders of anatase phase with high photocatalytic activity are prepared by a one-step hydrothermal strategy in a $NH_4HF_2-H_2O-C_2H_5OH$ mixed solution with tetrabutylorthotitanate ($Ti(OC_4H_9)_4$, TBOT) as precursor. The prepared samples are characterized by X-ray diffraction, X-ray photoelectron spectroscopy, N_2 adsorption−desorption isotherms, UV−vis absorption spectroscopy, and transmission electron microscopy. The production of hydroxyl radicals ($^{\bullet}OH$) on the surface of UV-illuminated TiO_2 is detected by a photoluminescence (PL) technique with use of terephthalic acid as a probe molecule. The photocatalytic activity is evaluated by photocatalytic oxidation decomposition of acetone in air under UV light illumination. The results show that the photocatalytic activity of $F-TiO_2$ powders is obviously higher than that of pure TiO_2 and commercial Degussa P25 (P25) powders due to the fact that the strong electron-withdrawing ability of the surface ≡Ti−F groups reduces the recombination of photogenerated electrons and holes, and enhances the formation of free OH radicals. Especially, the $F-TiO_2$ powder prepared at the nominal atomic ratio of fluorine to titanium (R_F) of 0.5 shows the highest photocatalytic activity and its rate constant k exceeds that of P25 by a factor of more than 3 times.

1. Introduction

In recent years, titanium dioxide and other semiconductor photocatalytic materials have been intensively investigated for their wide potential application in water and air purification and solar energy conversion since Fujishima and Honda discovered the photocatalytic splitting of water on TiO_2 electrodes in 1972.[1−11] Among the various oxide and nonoxide semiconductor photocatalysts, titania has proven to be the most suitable for widespread environmental applications due to its biological and chemical inertness, strong oxidizing power, cost-effectiveness, and long-term stability against photocorrosion and chemical corrosion. However, the photocatalytic performance of TiO_2 must be further enhanced from the practical use and commercial point of view.[12−14] For achieving this purpose, the surface properties of TiO_2 play a very important role in determining photocatalytic reaction efficiencies since heterogeneous photocatalytic reactions take place on the surface, which are related to various parameters such as composition, phase structures, surface hydroxyl group, particle size, crystallinity, surface defects, surface metal deposits, and adsorbates or surface complexes. TiO_2 surfaces have been actively modified through manipulating the above parameters to enhance the photocatalytic performance.[15−18]

Recently, fluorinated TiO_2 has been extensively investigated in relation to doping ($TiO_{2-x}F_x$)[19−25] or surface fluorination ($F-TiO_2$).[26−30] It has been found that fluoride doping enhances the crystallization of the anatase phase and the photocatalytic activity.[20−23] On the other hand, surface fluorination of TiO_2 has been used as a new method of surface modification.[31−34] Surface fluorination can be easily carried out by a simple ligand exchange reaction between surface hydroxyl groups on TiO_2 and fluoride anions (F^-).

$$\equiv Ti-OH + F^- \leftrightarrow \equiv Ti-F + OH^- \quad pK_F = 6.2 \text{ (ref 35)} \quad (1)$$

Surface-fluorinated TiO_2 ($F-TiO_2$) shows enhanced photocatalytic activities in aqueous suspensions for the photocatalytic oxidation (PCO) of Acid Orange 7 and phenol.[15,16] The extent of fluorination on TiO_2 highly depends on pH, showing a maximum (about 99%) around pH 3−4.[15] Minero et al.[27,28] examined the influence of fluoride-treated catalysts on the PCO of phenol in aqueous media and found that the PCO of phenol was enhanced with $F-TiO_2$ and proposed that the fluorinated surface favors the generation of free OH radicals (not surface-bound $^{\bullet}OH$), which are responsible for the enhanced oxidation. Since the surface fluorides themselves should not be reactive with valence band (VB) holes [$E°(F^{\bullet}/F^-) = 3.6$ V vs NHE].[15,30,36] The higher PCO rate in the $F-TiO_2$ suspension is ascribed to the enhanced generation of mobile free OH radicals (reaction 2) whereas most OH radicals generated on naked TiO_2 surface prefer to remain adsorbed (reaction 3).[15]

$$\equiv Ti-F + H_2O \text{ (or } OH^-) + h_{vb}^+ \rightarrow \equiv Ti-F + {}^{\bullet}OH_{free} + H^+ \quad (2)$$

$$\equiv Ti-OH + h_{vb}^+ \rightarrow \equiv Ti-OH^{\bullet+} \quad (3)$$

This suggests that the photocatalytic reactions in the $F-TiO_2$ suspension can occur in the solution bulk remote from the TiO_2 surface.[15] Choi and his colleagues have done a lot of related research work and further confirmed the above results, also indicating that hole mediated photocatalytic reactions are inhibited on the contrary because of the hindered adsorption of substrates on $F-TiO_2$.[15,18,31,32] In addition, they found that surface fluorination of TiO_2 enhanced the remote PCO at the

* To whom correspondence should be addressed. E-mail: jiaguoyu@yahoo.com.

10.1021/jp900136q CCC: $40.75
Published on Web 03/31/2009

air/catalyst interface by facilitating the desorption of OH radicals under UV irradiation (reaction 2).[29,33] Mrowetz and Selli also reported direct experimental evidence of the higher concentration of hydroxyl radicals generated on fluorinated titanium dioxide ($F-TiO_2$) under UV irradiation obtained by spin-trapping EPR measurements and the faster photoinduced bleaching of the azo dye Acid Red 1 (AR1) observed in the presence of $F-TiO_2$.[37,38] Indeed, the formation of $\equiv Ti-F$ species, which dominate at acidic pH, decreases the amount of surface hydroxyl groups, up to their almost complete displacement at pH 3.5−4.0. Significant variations of the semiconductor oxide photocatalytic behavior have consequently been observed.[39−42] On the other hand, Lewandowski and Ollis[30] reported that the PCO of aromatic air pollutants was unaffected (for toluene) or even inhibited (for benzene and *m*-xylene) by the surface fluorination of TiO_2. Judging from the results of previous studies, the effect of surface fluorination of TiO_2 could be either positive or negative depending on the kind of substrate and experimental conditions.

It is well-known that volatile organic compounds (VOCs) are triggering serious environmental problems such as stratospheric ozone depletion and tropospheric ozone increase, depending on their chemical structures.[43] Furthermore, some of these volatile organic compounds in the indoor air are also arousing health disorders, such as leukemia, nausea, headache, and fatigue.[44] Degradation of acetone in air is particularly important because it is one of the principle indoor air pollutants. As a result, PCO reactions of acetone with TiO_2 were frequently investigated.[45−47] In this study, mesporous surface-fluorinated anatase TiO_2 powders with high photocatalytic activity are prepared in one-step by hydrothermal treatment of precipitates of tetrabutylorthotitanate ($Ti(OC_4H_9)_4$, TBOT) in a $NH_4HF_2-H_2O-C_2H_5OH$ mixed solution. The influences of the concentration of NH_4HF_2 on surface microstructure and photocatalytic activity of TiO_2 are studied and discussed. This work is different from the previously reported work by Choi and Pelizzetti et al. because surface fluorination at ambient temperature does not affect the crystallinity of TiO_2 at all. Contrarily, hydrothermal surface fluorination treatment can enhance the crystallization of TiO_2.

2. Experimental Section

2.1. Sample Preparation. All chemicals used in this study were analytical grade and were used without further purification. Distilled water was used in all experiments. In a typical preparation procedure, 0.02 mol of TBOT was dissolved into 30 mL of ethanol and then this TBOT solution was added dropwise to 120 mL of the $NH_4HF_2-H_2O$ mixed solution under vigorous stirring at room temperature. The nominal atomic ratios of fluorine to titanium (R_F) were 0, 0.25, 0.5, and 1. The pH values of the corresponding mixed solution are about 7, 4, 3.5, and 2.5, respectively. The above suspensions were then transferred to 200-mL Teflon-lined autoclaves until 80% of their volume was filled. The autoclaves were sealed and maintained at 150 °C for 10 h. After this hydrothermal reaction, the white precipitates were collected, washed with distilled water followed by a rinse in ethanol, and then dried in an oven at 80 °C for 2 h.

2.2. Characterization. The X-ray diffraction (XRD) measurements, which were used to characterize the crystalline phase, phase composition, and crystallite size of the TiO_2 powders, were carried out by an X-ray diffractometer (type HZG41B-PC), using Cu Kα radiation at a scan rate of 0.05° 2θ s^{-1}. The accelerating voltage and the applied current were 40 kV and 80 mA, respectively. The X-ray photoelectron spectroscopy measurement (XPS) was made in an ultrahigh vacuum VG ESCALAB 210 electron spectrometer equipped with a multichannel detector. The spectra were excited with Mg Kα (1253.6 eV) radiation (operated at 200 W) of a twin anode in the constant analyzer energy mode with a pass energy of 30 eV. All the binding energies were referenced to the C 1s peak at 284.8 eV of the surface adventitious carbon. The morphologies of TiO_2 powders were observed by transmission electron microscopy (TEM) and high-resolution transmission electron microscopy (HRTEM), using a JEM-2100F electron microscope (JEOL, Japan) at an acceleration voltage of 200 kV. The brunauer−Emmett−Teller (BET) specific surface area (S_{BET}) of the powders was analyzed by nitrogen adsorption in a Micromeritics ASAP 2020 nitrogen adsorption apparatus (USA). All the as-prepared samples were degassed at 150 °C prior to nitrogen adsorption measurements. UV−vis diffused reflectance spectra of TiO_2 powders were obtained for the dry-pressed disk samples with a UV−vis spectrotometer (UV2550, Shimadzu, Japan). $BaSO_4$ was used as a reflectance standard in a UV−vis diffuse reflectance experiment.

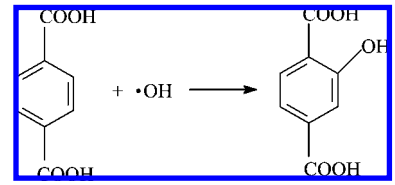

Figure 1. Formation of 2-hydroxyterephtalic acid due to the reaction between •OH and terephthalic acid.

2.3. Analysis of Hydroxyl Radicals (•OH). The formation of hydroxyl radicals (•OH) on the surface of UV-illuminated TiO_2 is detected by a photoluminescence (PL) technique with terephthalic acid as a probe molecule. Terephthalic acid readily reacts with •OH to produce highly fluorescent product, 2-hydroxyterephthalic acid (as shown in Figure 1).[48,49] This technique has been used in radiation chemistry, sonochemistry, and biochemistry[50−58] for the detection of •OH generated in water. The intensity of the PL peak of 2-hydroxyterephtalic acid is in proportion to the amount of OH radicals produced in water.[48,49] The optimal concentration of terephthalic acid solution was about 5×10^{-4} M in a diluted NaOH aqueous solution (2×10^{-3} M). The results of Hashimoto et al. further indicated that the hydroxylation reaction of terephthalic acid proceeds mainly in the concentration range of $10^{-3}-10^{-4}$ M.[48] This method relies on the PL signal at 425 nm of the hydroxylation of terephthalic acid with •OH generated at the water/TiO_2 interface. The method is rapid, sensitive, and specific, needing only simple standard PL instrumentation.

Experimental procedures are as follows: At ambient temperature, 0.1 g of TiO_2 powder sample is dispersed in a 20 mL of the 5×10^{-4} M terephthalic acid aqueous solution with a concentration of 2×10^{-3} M NaOH in a dish with a diameter of about 9.0 cm. A 15 W, 365 nm UV lamp (6 cm above the dishes) (Cole-Parmer Instrument Co., USA) is used as a light source. Integrated light intensity measured with a UV radiometer (UV-A) was 2.9 mW/cm^2 (the peak intensity of 365 nm). PL spectra of the generated 2-hydroxyterephthalic acid were measured on a Hitachi F-7000 fluorescence spectrophotometer. After UV irradiation every 15 min, the reaction solution was filtrated to measure the increase in the PL intensity at 425 nm excited by 315 nm light of 2-hydroxyterephthalic acid.

2.4. Evaluation of Photocatalytic Activity. The photocatalytic activity of the naked and fluorinated TiO_2 powders was

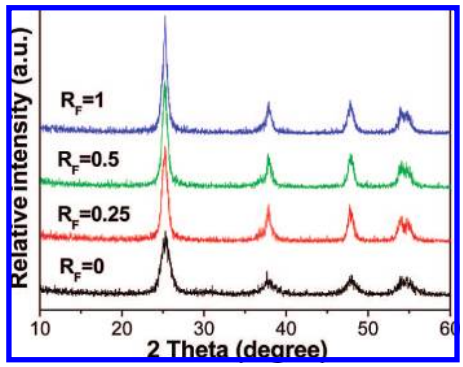

Figure 2. XRD patterns of the TiO_2 samples prepared from the $NH_4HF_2-H_2O-C_2H_5OH$ mixed solutions with varying $R_F = 0$ (pure water), 0.25, 0.5, and 1.

measured for the PCO of acetone under UV light irradiation at ambient temperature with a 15 L reactor. The photocatalysts were prepared by coating an aqueous suspension of TiO_2 powders onto three dishes with diameters of 7.0 cm. The weight of the photocatalyst used for each experiment was kept at about 0.3 g. The TiO_2 photocatalysts were dried in an oven at 80 °C for about 2 h to evaporate the water and then cooled to room temperature before use. After the dishes coated with TiO_2 powder photocatalysts were placed in the reactor, a small amount of acetone was injected into the reactor with a microsyringe. The acetone vapor was allowed to reach adsorption and desorption equilibrium with the catalyst in the reactor prior to UV light irradiation. The analysis of acetone, carbon dioxide, and water vapor concentration in the reactor was conducted on line with a Photoacoustic IR Multigas Monitor (INNOVA Air Tech Instruments Model 1412).[59−61] The initial concentration of acetone after the adsorption equilibrium was about 300 ppm, which remained constant for about 5 min until a 15 W, 365 nm UV lamp (6 cm above the dishes) (Cole-Parmer Instrument Co., USA) in the reactor was switched on. Integrated UV intensity in the wavelength range of 310−400 nm striking the samples measured with a UV radiometer (Model UV-A, made in Photoelectric Instrument Factory of Beijing Normal University) was 2.9 mW/cm^2, while the peak wavelength of UV light was 365 nm. Each set of experiments was followed for 60 min. The photocatalytic activity of the powders can be quantitatively evaluated by comparing the apparent reaction rate constants. The PCO of acetone is a pseudo-first-order reaction and its kinetics may be expressed as follows: $\ln(C_0/C) = kt$,[20] where k is the apparent reaction rate constant, and C_0 and C are the initial concentration and the reaction concentration of acetone, respectively.

3. Results and Discussion

3.1. Phase Structures. The phase structure, crystallite size, and crystallinity of TiO_2 are of great importance for its photocatalytic activity. XRD was used to investigate the changes of phase structures and crystallite sizes of the naked and fluorinated-TiO_2 samples. Figure 2 shows the effects of R_F on phase structures of the TiO_2 samples prepared from $NH_4HF_2-H_2O-C_2H_5OH$ mixed solution with varying R_F. The anatase phase is dominant in the as-prepared sample from pure water [JCPDS No. 21-1272, space group $I4_1/amd$ (141)], but there is a small amount of brookite phase found in it ($R_F = 0$). The minor peak at $2\theta = 30.7°$ corresponds to the (121) plane diffraction of the brookite phase of titania [JPCDS No. 29-1360, space group *Pcab* (61)]. The diffraction peak of the brookite disappears in the presence of NH_4HF_2. It can be concluded that

TABLE 1: Effects of R_F on Phase Structure, BET Surface Areas, and Pore Parameters of Titania Powders

R_F	phase content[a]	crystalline size (nm)	S_{BET} (m^2/g)	av pore size	pore vol (cm^3/g)	porosity (%)	rel crystallinity
0	A, B	8.1 (A)	196.6	5.7	0.28	50.9	1
0.25	A	10.9 (A)	126.6	5.8	0.19	41.3	1.35
0.5	A	11.2 (A)	122.0	6.1	0.19	41.3	1.38
1	A	11.5 (A)	120.9	6.2	0.18	40.0	1.42

[a] A and B denote anatase and brookite, respectively.

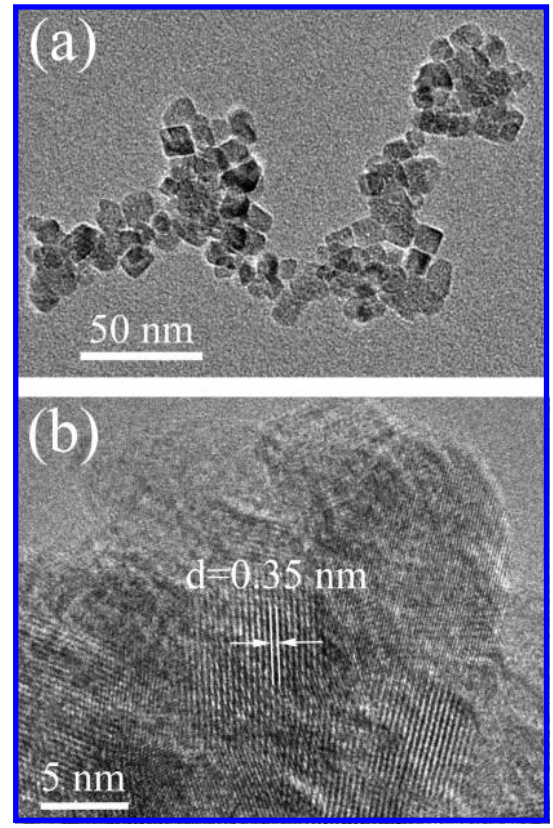

Figure 3. TEM (a) and HRTEM images (b) of the fluorinated TiO_2 sample ($R_F = 0.5$).

NH_4HF_2 inhibits the formation of the brookite phase. Further observation shows that with increasing R_F, XRD peak intensities of anatase steadily become stronger and the width of XRD diffraction peaks of anatase becomes slightly narrower, indicating the formation of greater TiO_2 crystallites and an enhancement of crystallization. The crystallinity of TiO_2 nanoparticles was quantitatively evaluated via the relative intensity of the (101) diffraction peak of the anatase.[62,63] Table 1 lists the average crystalline sizes and relative anatase crystallinity of TiO_2 samples prepared at different R_F. It can be seen that the average crystalline sizes and relative anatase crystallinity increase with increasing R_F. This is in good agreement with our previous reported results. The F^- not only suppresses the formation of brookite but also enhances the crystallization of the anatase phase and promotes crystallite growth by adsorbing on the surface of TiO_2 particles.[20,21,64]

The microstructure of fluorinated TiO_2 powders was further studied by TEM and HRTEM. Figure 3a shows the TEM image of the fluorinated TiO_2 powders prepared at $R_F = 0.5$. It can be observed from Figure 3a that the nanocrystallite appears in an agglomerated status, and mesoporous structures appear with a nonorder status. The size of the primary particles estimated from the TEM image was about 11 ± 2 nm, which was in good agreement with the value (11.2 nm) calculated from the XRD

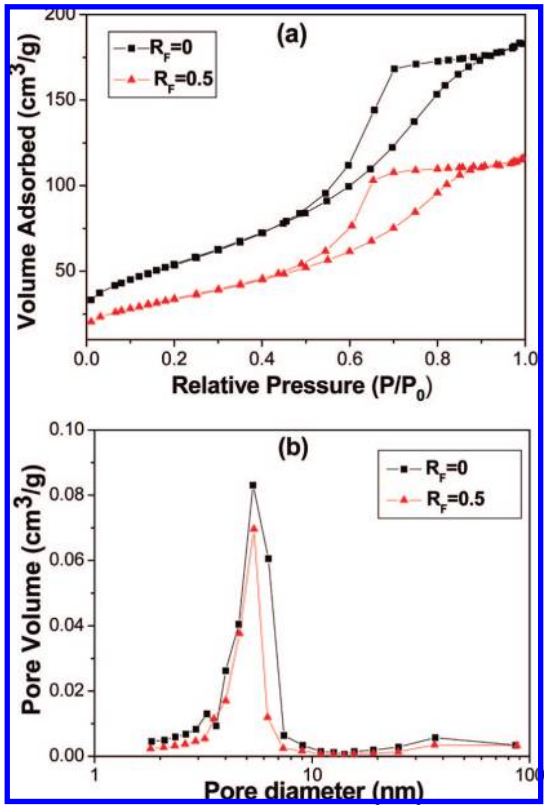

Figure 4. Nitrogen adsorption−desorption isotherms (a) and corresponding pore size distribution curves (b) calculated from the desorption branch of the nitrogen isotherm by the BJH method of the naked and fluorinated TiO_2 samples prepared at $R_F = 0$ and 0.5, respectively.

pattern by using the Scherrer equation (as shown in Table 1). Figure 3b shows the corresponding HRTEM image of the fluorinated TiO_2 sample. It shows clear lattice fringes, which allowed for the identification of crystallographic spacing. The fringe spacing of ca. 0.35 nm matches that of the (101) crystallographic plane of TiO_2 anatase.[63]

3.2. BET Surface Areas and Pore Distributions. Figure 4 shows nitrogen adsorption−desorption isotherms and the corresponding pore size distribution curves of the naked and fluorinated TiO_2 samples. It can be seen from Figure 4a that the naked and fluorinated TiO_2 powders have isotherms of type IV and one hysteresis loop at a relative pressure range of 0.5 to 0.8. The hysteresis loops are of type H2, which can be observed in the ink-bottle-like pores with narrow necks and wider bodies.[65−67] The relative-presure position of two isotherms has no obvious difference besides different adsorbed volume. The pore size distribution calculated from the desorption branch of the nitrogen isotherm by the BJH (Barrett−Joyner−Halenda) method shows a narrow range of 3.0−8.0 nm with a maximum pore diameter of about 5.4 nm (see Figure 4b).[65] These mesopores are from the aggregation of primary particles. The narrow pore distributions also imply that the prepared naked and fluorinated TiO_2 particles have a uniform particle size distribution.

Table 1 also shows that all samples have mesoporous structures with an average pore size of about 6 nm. These mesopores enhance the rate of gaseous photocatalytic reaction due to rapid diffusion of various gaseous molecules within mesopores during photocatalytic reaction. It can be seen from Table 1 that in pure water, the as-prepared TiO_2 powders show the largest S_{BET} value of 196.6 $m^2\ g^{-1}$. However, the surface area, pore volume, and porosity decrease in the presence of F^- ions, while the pore diameter increases due to the growth of TiO_2 crystallites.

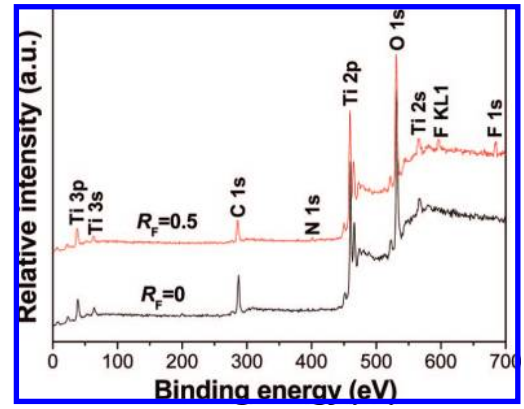

Figure 5. XPS survey spectra of the naked and fluorinated TiO_2 samples prepared at $R_F = 0$ and 0.5, respectively.

3.3. XPS Analysis. Figure 5 shows XPS survey spectra of the naked and fluorinated TiO_2 samples prepared at $R_F = 0$ and 0.5, respectively. The naked TiO_2 sample contains Ti, O, and C elements, with sharp photoelectron peaks appearing at binding energies of 458 (Ti2p), 531 (O1s), and 285 eV (C1s). The carbon peak is attributed to the residual carbon from the sample and adventitious hydrocarbon from the XPS instrument itself. On the contrary, the fluorinated TiO_2 sample contains not only Ti, O, and C, but also a small amount of F and N elements (binding energies at 684 and 400 eV, respectively), which come from the precursor NH_4HF_2.

Figure 6a shows the high-resolution XPS spectrum of the F 1s region, taken on the surface of the fluorinated TiO_2 powders prepared at $R_F = 0.5$. According to our previous results as well as those of Choi et al.,[15,20] the F1s peak at 684 eV is due to the surface fluoride (≡Ti−F) formed by ligand exchange reaction between F^- and the surface hydroxyl group on the surface of TiO_2. No signal of F^- ions in the lattice (BE = 688.5 eV) was found.[20,68−70] This indicates that the surface fluorination of TiO_2 readily takes place at an acidic hydrothermal environment (pH 2−4), which prevents the substitution of F^- for O^{2-} in the lattice of TiO_2. This is not difficult to understand because the hydrothermal environment can accelerate crystallization of TiO_2 based on the in situ dissolution−recrystallization process and reduced defects and impurity in TiO_2.[71] Therefore, we can obtain anatase-phase TiO_2 with high surface fluorination in an acidic environment at a relatively low temperature. Figure 6b shows the corresponding high-resolution XPS spectrum of the N1s region taken from the sample prepared at $R_F = 0.5$. The N1s peak at 400.4 eV is assigned to some N elements adsorbed on the surface of TiO_2.[44,68,70,72] No incorporated N elements in the titania lattice were found.[70,72] The exact amounts of F and N elements in F−TiO_2 ($R_F = 0.5$) were characterized by XPS and their atomic percentages respectively are 3.94% and 1.85%, which are not in agreement with that of the precursor solution. This is easy to understand because F and N elements only adsorbed on the surface of F−TiO_2.

Figure 7 shows UV−vis absorption spectra of the naked and fluorinated TiO_2 samples prepared at $R_F = 0$ and 0.5, respectively. The UV−vis absorption of the fluorinated TiO_2 sample is slightly higher than that of the naked TiO_2 sample at <500 nm, whereas the absorption edge region is almost unaffected by the surface fluorination or nitrification. This also further confirms that F and N elements do not enter the lattice of TiO_2.

3.4. Hydroxyl Radical Analysis. The PL emission spectra excited at 315 nm from terephthalic acid solution were measured

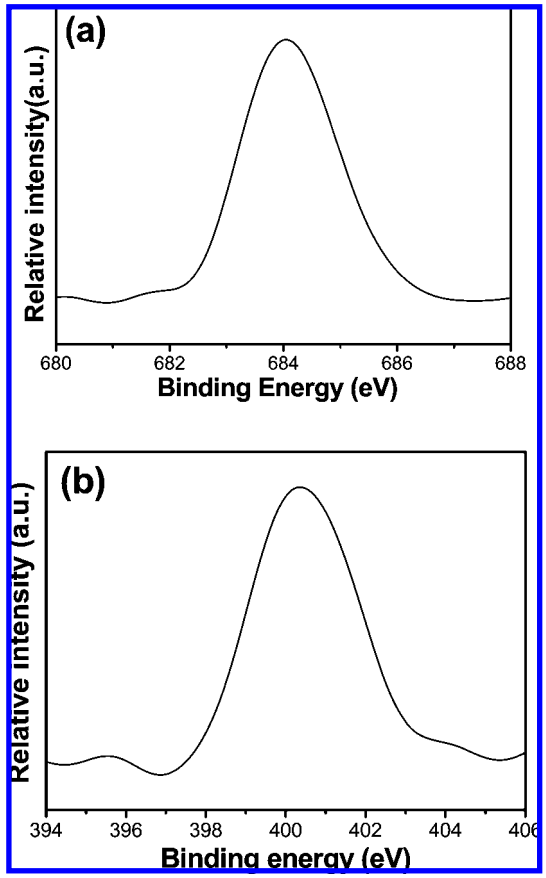

Figure 6. High-resolution XPS spectra of F 1s (a) and N 1s (b) of the fluorinated TiO_2 sample prepared at $R_F = 0.5$.

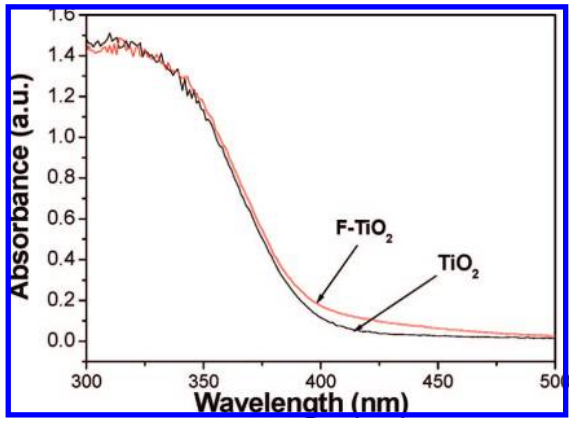

Figure 7. UV−vis absorption spectra of the naked and fluorinated TiO_2 samples prepared at $R_F = 0$ and 0.5, respectively.

every 15 min of illumination. Figure 8 shows the changes of PL spectra from 5×10^{-4} M terephthalic acid solution in 2×10^{-3} M NaOH with irradiation time. It can be seen that a gradual increase in PL intensity at about 425 nm is observed with increasing irradiation time. However, no PL increase was observed in the absence of UV light or TiO_2 samples This suggests that the fluorescence is caused by chemical reactions of terephthalic acid with $^{\bullet}OH$ formed on the TiO_2/water interface via photocatalytic reactions.[48,49]

Figure 9 shows the plots of increase in PL intensity at 425 nm against irradiation time. The PL intensity by UV irradiation in terephthalic acid solutions increased linearly against time. Consequently, it can be inferred that OH radicals produced at the TiO_2 surface are in proportion to the light irradiation time obeying zero-order reaction rate kinetics.[48,49] The formation rate

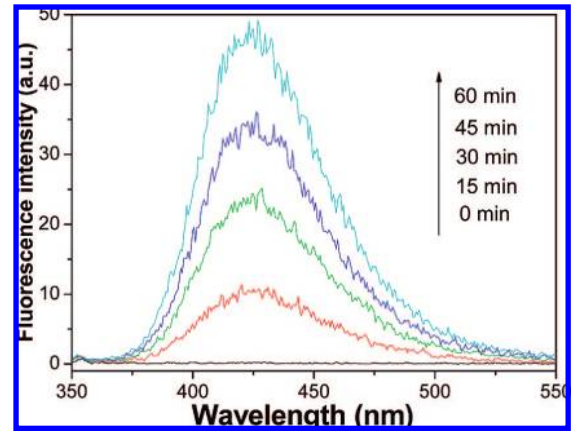

Figure 8. PL spectral changes observed during irradiation of the fluorinated TiO_2 sample prepared at $R_F = 0.5$ in a 5×10^{-4} M basic solution of terephthalic acid (excitation at 315 nm). Each fluorescence spectrum was recorded every 15 min of UV illumination.

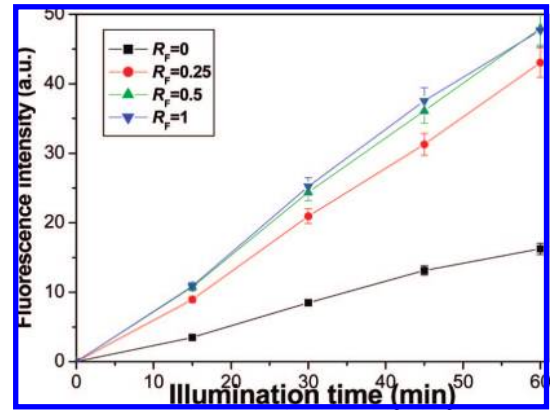

Figure 9. Plots of the induced PL intensity at 426 nm against irradiation time for terephthalic acid on the naked and fluorinated TiO_2 samples prepared at $R_F = 0$, 0.25, 0.5, and 1.

of the OH radicals could be expressed by the slop of these lines shown in Figure 9. It can be easily seen that the formation rate of OH radicals on the fluorinated TiO_2 powders is much larger than that of the naked TiO_2 powders. This suggests that the surface fluorination of TiO_2 enhances the production of OH radicals. Why can surface fluorination enhance the formation of OH radicals? One possible explanation is that most OH radicals generated on naked TiO_2 surface prefer to remain adsorbed on the surface of TiO_2 (reaction 3); however, the OH radicals on F−TiO_2 surface are free mobile (reaction 2).[15] Therefore, it is not surprising that the OH radicals are generated on F−TiO_2 is much faster than on the naked TiO_2. Another cause is that fluorine is the most electronegative element: it is adsorbed on the surfaces of TiO_2 and can attract the photogenerated electrons and then reduce the recombination rate of the photogenerated electrons and holes. The formation rate of free OH radicals in water is, therefore, enhanced. This PL result also further confirmed Choi and Pelizzetti et al.'s results.[15,27,28] Figure 9 indicates that with further increasing R_F, the formation rate of OH radicals slightly increases.

3.5. Photocatalytic Activity. Many investigations have shown that surface fluorination is an effective treatment method to enhance the photoactivity and crystallization of nanosized TiO_2 photocatalysts.[15,26−28] The photocatalytic activity of the naked and fluorinated TiO_2 powders was evaluated by the photocatalytic degradation of acetone in air. Figure 10 shows a comparison of photocatalytic activity of the naked and fluori-

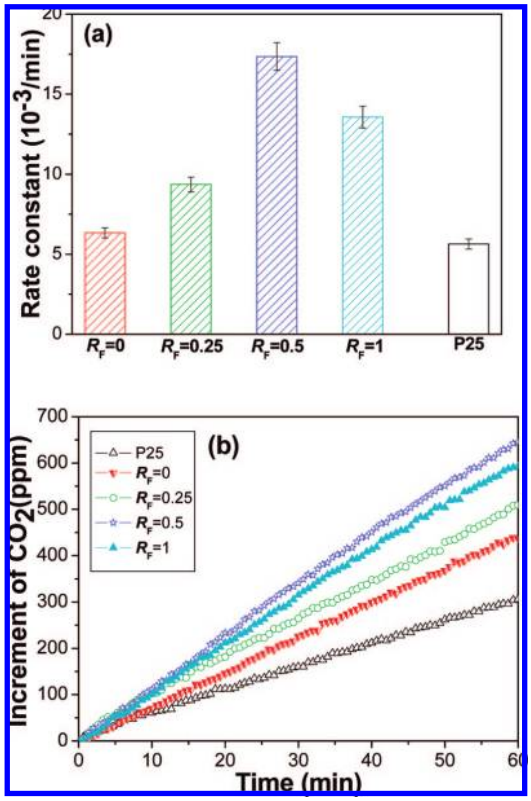

Figure 10. (a) Comparison of photocatalytic activity of the naked and fluorinated TiO_2 samples prepared at $R_F = 0$, 0.25, 0.5, and 1 and Degussa P25 for photocatalytic decomposition of acetone. (b) The dependence of corresponding produced CO_2 concentration (ppm) on R_F.

nated TiO_2 samples and Degussa P25. For the naked TiO_2 sample prepared in pure water, it shows a good photocatalytic activity. Its k reaches 6.33×10^{-3}. This is assigned to its high specific surface areas and small crystallite size. The activity of all fluorinated TiO_2 powders is higher than that of the naked ones and P25. With increasing R_F, the photocatalytic activity of fluorinated TiO_2 powder significantly increased due to the enhancement of crystallization of TiO_2 (as shown in Figure 2 and Table 1). At $R_F = 0.5$, the k reaches the highest value and its value was 17.35×10^{-3}. The k was determined to be 5.64×10^{-3} for Degussa P-25 (P25), which is well-known to have excellent photocatalytic activity.[73] The photocatalytic activity of the fluorinated TiO_2 powders prepared at $R_F = 0.5$ exceeded that of P25 by a factor of 3.01, which is attributed to the fact that F−TiO_2 had larger specific surface areas, smaller crystallite size and mesoporous structures, etc. Usually, the specific surface areas and crystallite size of P25 are about 50 $m^2\ g^{-1}$ and 30 nm, respectively. With further increasing R_F values, the k decreases drastically.

The photocatalytic reactions of semiconductor surface are due to the production of photogenerated electrons and holes in the semiconductors by the absorption of UV light. These electron and hole carriers are unstable, however, and recombination of the photogenerated electrons and holes can occur very quickly, dissipating the input energy as heat. In fact, the photocatalytic efficiency depends on the recombination rate or lifetime of photogenerated electrons and holes. If recombination occurs too fast, then there is not enough time for any other chemical reactions to occur. Why is the photocatalytic activity of all F−TiO_2 powders higher than that of the naked TiO_2 powders? One possible explanation for this photocatalytic activity enhancement is that the surface ≡Ti−F group can act as an electron-trapping site to trap the photogenerated electrons by tightly holding trapped electrons due to the strong electronegativity of the fluorine and then transferring them to O_2 adsorbed on the surface of TiO_2 (see Figure 11). This is also similar to our previous suggestion that trifluoroacetate (carrying a strongly electron withdrawing CF_3 group) complexed on TiO_2 surface could trap CB electrons with reduction of the charge-pair recombination.[15,26] Therefore, the existence of a certain amount of F^- ions on the surface of TiO_2 results in the reduction of the recombination rate of electron and hole and enhancement of photocatalytic activity. One direct evidence is the formation rate of free OH radicals on F−TiO_2 is much greater than that of surface-bound OH radicals on TiO_2 (see Figure 9). Also, the redox potential of free OH radicals in solution (ca. 2.3 V vs NHE at pH 7) is larger than that of surface-adsorbed OH radicals on TiO_2 (about 1.5−1.7 V vs NHE at pH 7).[34,74−76]

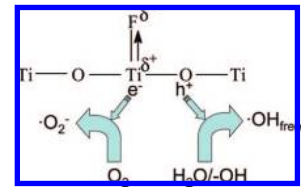

Figure 11. Schematic diagram for generation and transfer of charge carriers in F−TiO_2 under UV irradiation.

The detailed charge carrier transfer processes on F−TiO_2 are as follows:

$$F{-}TiO_2 + h\nu \rightarrow h^+ + e^- \quad \text{electron and hole generation} \tag{4}$$

$$F{-}Ti^{4+} + e^- \rightarrow F{-}Ti^{3+} \tag{5}$$

$$O^{2-} + h^+ \rightarrow O^- \tag{6}$$

$$F - Ti^{3+} + O_2 \rightarrow F - Ti^{4+} + {}^{\bullet}O_2^- \quad \text{electron release} \tag{7}$$

$$O^- + OH^- \text{ (or } H_2O) \rightarrow O^{2-} + {}^{\bullet}OH \quad \text{hole release} \tag{8}$$

It should be noted that this enhancement method for photocatalytic activity is different from our previous study on preparation of F^--doped TiO_2 solid solution $TiO_{2-x}F_x$ and trifluoroacetic acid (TFA) surface modification of TiO_2.[20,26] The former is due to the fact that F^--doping converts Ti^{4+} to Ti^{3+} by charge compensation and the existence of Ti^{3+} can reduce the electron−hole recombination rate, and subsequently enhances the photocatalytic activity.[20] The latter is ascribed to the fact that the TFA complex bound on the surface of TiO_2 acts as an electron scavenger and, thus, reduces the recombination of photogenerated electrons and holes. This activity enhancement is only temporary, however, since the TFA eventually decomposes under the strong oxidizing environment of photocatalysis.[26] On the contrary, in this study, the enhanced photocatalytic activity of F−TiO_2 is lasting because the surface fluorides themselves cannot react with valence band (VB) holes (3.0 V) [$E^\circ(F^\bullet/F^-) = 3.6$ V vs NHE].[15,20,30]

The above results indicate that the introduction of F^- ions on the surface of TiO_2 is responsible for a reduction of the recombination rate of photogenerated electrons and holes,

resulting in the enhancement of photoactivity. Moreover, a decrease in the activity is observed when the concentration of F^- ions becomes larger. This indicates that the photocatalytic activity of $F-TiO_2$ is strongly dependent on the dopant concentration since the F^- ions can serve not only as a mediator of interfacial charge transfer but also as a recombination center. In our case an optimal dopant concentration is 0.5 atom %. Above that concentration, F^- ions steadily become recombination centers and the activity steadily decreases. However, with increasing R_F, the formation rate of OH radicals on $F-TiO_2$ always increases. This indicates that the formation rate of OH radicals is an important factor influencing photocatalytic activity, but is not the only factor. Some other factors such as specific surface areas and the dopant concentration also have great influence on photoactivity. Moreover, The PCO of acetone is carried out in the gasous phase; however, the detection of OH radicals is done in solution. Of course, a detailed mechanism study needs to be performed.

4. Conclusions

Mesporous fluorinated anatase TiO_2 powders with high photocatalytic activity could be prepared in one step by a simple hydrothermal strategy. The surface fluorination exhibits a significant influence on the crystallinity, crystallite size, phase structure, and photocatalytic activity of the TiO_2 powders. F^- ions suppress the crystallization of the brookite phase, catalyze the phase transformation of brookite to anatase, and enhance the growth of anatase crystallites by adsorbing on the surface of TiO_2. The activity of all fluorinated TiO_2 powders is higher than that of the naked ones. This is due to the strong electron-withdrawing ability of the surface $\equiv Ti-F$ groups to reduce the recombination of photogenerated electrons and holes, meanwhile enhancing the production of free OH radicals. With increasing R_F, the photocatalytic activity of fluorinated TiO_2 powder significantly increases due to the enhancement of crystallization of TiO_2. At $R_F = 0.5$, the rate constant k of the sample reaches the highest value and its value exceeded that of P25 by a factor of about 3 times.

Acknowledgment. This work was partially supported by the National Natural Science Foundation of China (50625208, 20773097, and 20877061). This work was also financially supported by the National Basic Research Program of China (2007CB613302 and 2009CB939704).

References and Notes

(1) Fujishima, A.; Honda, K. *Nature (London)* **1972**, *238*, 37.
(2) Fox, M. A.; Dulay, M. T. *Chem. Rev.* **1993**, *93*, 341.
(3) Hoffmann, M. R.; Martin, S. T.; Choi, W.; Bahnemann, D. W. *Chem. Rev.* **1995**, *95*, 69.
(4) Yu, J. G.; Yu, H. G.; Guo, H. T.; Li, M.; Mann, S. *Small* **2008**, *4*, 87.
(5) Gratzel, M. *Inorg. Chem.* **2005**, *44*, 6841.
(6) Li, X. Z.; Li, F. B. *Environ. Sci. Technol.* **2001**, *35*, 2381.
(7) Fujishima, A.; Rao, T. N.; Tryk, D. A. *J. Photochem. Photobiol. C* **2000**, *1*, 1.
(8) Yu, J. G.; Yu, X. X. *Environ. Sci. Technol.* **2008**, *42*, 4902.
(9) Yu, J. G.; Liu, S. W.; Yu, H. G. *J. Catal.* **2007**, *249*, 59.
(10) Park, J. H.; Kim, S.; Bard, A. J. *Nano Lett.* **2006**, *6*, 24.
(11) Wu, Y. Q.; Lu, G. X.; Li, S. B. *J. Photochem. Photobiol. A* **2006**, *181*, 263.
(12) Yu, J. G.; Yu, H. G.; Cheng, B.; Zhao, X. J.; Yu, J. C.; Ho, W. K. *J. Phys. Chem. B* **2003**, *107*, 13871.
(13) Ksibi, M.; Rossignol, S.; Tatibouet, J. M.; Trapalis, C. C. *Mater. Lett.* **2008**, *62*, 4204.
(14) Frank, S. N.; Bard, A. J. *J. Am. Chem. Soc.* **1977**, *99*, 303.
(15) Park, H.; Choi, W. *J. Phys. Chem. B* **2004**, *108*, 4086.
(16) Choi, W. *Catal. Surv. Asia* **2006**, *10*, 16.
(17) Kamat, P. V. *Chem. Rev.* **1993**, *93*, 267.
(18) Vohra, M. S.; Kim, S.; Choi, W. *J. Photochem. Photobiol. A* **2003**, *160*, 55.
(19) Subbarao, S. N.; Yun, Y. H.; Kershaw, R.; Dwight, K.; Wold, A. *Inorg. Chem.* **1979**, *18*, 488.
(20) Yu, J. C.; Yu, J. G.; Ho, W. K.; Jiang, Z. T.; Zhang, L. Z. *Chem. Mater.* **2002**, *14*, 3808.
(21) Yu, J. G.; Yu, J. C.; Cheng, B.; Hark, S. K.; Iu, K. *J. Solid State Chem.* **2003**, *174*, 372.
(22) Hattori, A.; Yamamoto, M.; Tada, H.; Ito, S. *Chem. Lett.* **1998**, 707.
(23) Hattori, A.; Shimoda, K.; Tada, H.; Ito, S. *Langmuir* **1999**, *15*, 5422.
(24) Wang, C. M.; Mallouk, T. E. *J. Phys. Chem.* **1990**, *94*, 423.
(25) Wang, C. M.; Mallouk, T. E. *J. Phys. Chem.* **1990**, *94*, 4276.
(26) Yu, J. C.; Ho, W. K.; Yu, J. G.; Hark, S. K.; Iu, K. *Langmuir* **2003**, *19*, 3889.
(27) Minero, C.; Mariella, G.; Maurino, V.; Pelizzetti, E. *Langmuir* **2000**, *16*, 2632.
(28) Minero, C.; Mariella, G.; Maurino, V.; Vione, D.; Pelizzetti, E. *Langmuir* **2000**, *16*, 8964.
(29) Park, J. S.; Choi, W. *Langmuir* **2004**, *20*, 11523.
(30) Lewandowski, M.; Ollis, D. F. *J. Catal.* **2003**, *217*, 38.
(31) Kim, H.; Choi, W. *Appl. Catal., B* **2007**, *69*, 127.
(32) Ryu, J.; Choi, W. *Environ. Sci. Technol.* **2004**, *38*, 2928.
(33) Park, J. S.; Choi, W. *Chem. Lett.* **2005**, *34*, 1630.
(34) Xu, Y. M.; Lv, K. L.; Xiong, Z. G.; Leng, W. H.; Du, W. P.; Liu, D.; Xue, X. J. *J. Phys. Chem. C* **2007**, *111*, 19024.
(35) Herrmann, M.; Kaluza, U.; Bohem, H. P. Z. *Anorg. Chem.* **1970**, *372*, 308.
(36) Wardman, P. *J. Phys. Chem.* **1989**, *18*, 1637.
(37) Mrowetz, M.; Selli, E. *Phys. Chem. Chem. Phys.* **2005**, *7*, 1100.
(38) Mrowetz, M.; Selli, E. *New J. Chem.* **2006**, *30*, 108.
(39) Oh, Y. C.; Jenks, W. S. *J. Photochem. Photobiol. A* **2003**, *161*, 69.
(40) Sanchez, J.; Augustynski, J. *J. Electroanal. Chem.* **1979**, *103*, 423.
(41) Chiang, K.; Amal, R.; Tran, T. *J. Mol. Catal. A* **2003**, *193*, 285.
(42) Oh, Y. C.; Bao, Y.; Jenks, W. S. *J. Photochem. Photobiol. A* **2004**, *164*, 323.
(43) Einaga, H.; Ibusuki, T.; Futamura, S. *Environ. Sci. Technol.* **2004**, *38*, 285.
(44) Yu, J. G.; Zhou, M. H.; Cheng, B.; Zhao, X. J. *J. Mol. Catal. A* **2006**, *246*, 176.
(45) Yu, J. G.; Liu, S. W.; Zhou, M. H. *J. Phys. Chem. C* **2008**, *112*, 2050.
(46) Zhao, J.; Yang, X. D. *Build. Environ.* **2003**, *38*, 645.
(47) Maira, A. J.; Yeung, K. L.; Soria, J.; Coronado, J. M.; Belver, C.; Lee, C. Y. *Appl. Catal., B* **2001**, *29*, 327.
(48) Ishibashi, K.; Fujishima, A.; Watanabe, T.; Hashimoto, K. *Electrochem. Commun.* **2000**, *2*, 207.
(49) Xiao, Q.; Si, Z. C.; Zhang, J.; Xiao, C.; Tan, X. K. *J. Hazard. Mater.* **2008**, *150*, 62.
(50) Collins, A. K.; Makrigiorgos, G. M.; Svensson, G. K. *Med. Phys.* **1994**, *21*, 1741.
(51) Khan, H. M.; Anwar, M.; Ahmad, G. *J. Radioanal. Nucl. Chem. Lett.* **1995**, *200*, 521.
(52) Matthews, R. W. *Radiat. Res.* **1980**, *83*, 27.
(53) Ashawa, S. C.; Kini, U. R.; Madhvanath, U. *Int. J. Appl. Radiat. Isot.* **1979**, *30*, 7.
(54) Armstrong, W. A.; Facey, R. A.; Grant, D. W.; Humphreys, W. G. *Can. J. Chem.* **1963**, *41*, 1575.
(55) Price, G. J.; Lenz, E. J. *Ultrasonics* **1993**, *31*, 451.
(56) Mason, T. J.; Lorimer, J. P.; Bates, D. M.; Zhao, Y. *Ultrason. Sonochem.* **1994**, *1*, S91.
(57) Fang, X.; Mark, G.; Sonntag, C. *Ultrason. Sonochem.* **1996**, *3*, 57.
(58) Makrigiorgos, G. M.; Baranowska-Kortylewicz, J.; Bump, E.; Sahu, S. K.; Berman, R. M.; Kassis, A. I. *Int. J. Radiat. Biol.* **1993**, *63*, 445.
(59) Yu, J. G.; Su, Y. R.; Cheng, B. *Adv. Funct. Mater.* **2007**, *17*, 1984.
(60) Zhou, M. H.; Yu, J. G.; Cheng, B. *J. Hazard. Mater. B* **2006**, *137*, 1838.
(61) Yu, J. G.; Zhang, L. J.; Cheng, B.; Su, Y. R. *J. Phys. Chem. C* **2007**, *111*, 10582.
(62) Yu, J. G.; Zhou, M. H.; Cheng, B.; Yu, H. G.; Zhao, X. J. *J. Mol. Catal. A* **2005**, *227*, 75.
(63) Yu, J. G.; Wang, G. H.; Cheng, B.; Zhou, M. H. *Appl. Catal., B* **2007**, *69*, 171.
(64) Kim, S.; Choi, W. *J. Phys. Chem. B* **2005**, *109*, 5143.
(65) Sing, K. S. W.; Everett, D. H.; Haul, R. A. W.; Moscou, L.; Pierotti, R. A.; Rouquerol, J.; Siemieniewska, T. *Pure Appl. Chem.* **1985**, *57*, 603.
(66) Gregg, S. J.; Sing, K. S. W. *Adsorption, Surface Area and Porosity*; Academic Press: London, UK, 1982.

(67) Yu, J. G.; Yu, J. C.; Leung, M. K. P.; Ho, W. K.; Cheng, B.; Zhao, X. J.; Zhao, J. C. *J. Catal.* **2003**, *217*, 69.
(68) Li, D.; Haneda, H.; Hishita, S.; Ohashi, N. *Chem. Mater.* **2005**, *17*, 2588.
(69) Huang, D. G.; Liao, S. J.; Liu, J. M.; Dang, Z.; Petrik, L. *J. Photochem. Photobiol. A* **2006**, *184*, 282.
(70) Li, D.; Haneda, H.; Hishita, S.; Ohashi, N.; Labhsetwar, N. K. *J. Fluorine Chem. Mater.* **2005**, *126*, 69.
(71) Yu, J. G.; Guo, H. T.; Davis, S. A.; Mann, S. *Adv. Funct. Mater.* **2006**, *16*, 2035.
(72) Zhou, M. H.; Yu, J. G. *J. Hazard. Mater.* **2008**, *152*, 1229.
(73) Yu, J. G.; Su, Y. R.; Cheng, B.; Zhou, M. H. *J. Mol. Catal. A* **2006**, *258*, 104.
(74) Lawless, D.; Serpone, N.; Meisel, D. *J. Phys. Chem.* **1991**, *95*, 5166.
(75) Tojo, S.; Tachikawa, T.; Fujitsuka, M.; Majima, T. *Chem. Phys. Lett.* **2004**, *384*, 312.
(76) Shriver, D. F.; Atkins, P. W.; Langford, C. H. *Inorganic Chemistry*, 2nd ed.; Oxford University Press: New York, 1996; p 407.

JP900136Q